

Supervised Fuzzy Partitioning

Pooya Ashtari ^{*a}, Fateme Nateghi ^{†b}, and Hamid Beigy ^{‡c}

^a*Department of Electrical Engineering, Sharif University of Technology, Tehran, Iran*

^b*Department of Biomedical Engineering, Amirkabir University of Technology, Tehran, Iran*

^c*Department of Computer Engineering, Sharif University of Technology, Tehran, Iran*

April 6, 2022

Abstract

Centroid-based methods including k-means and fuzzy c-means are known as effective and easy-to-implement approaches to clustering purposes in many areas of application. However, these algorithms cannot be directly applied to supervised tasks. We propose a generative model extending the centroid-based clustering approach to be applicable to classification tasks. Given an arbitrary loss function, our approach, termed Supervised Fuzzy Partitioning (SFP), incorporates labels information into its objective function through a surrogate term penalizing the empirical risk. We also fuzzify the partition and assign weights to features alongside entropy-based regularization terms, enabling the method to capture more complex patterns, to identify significant features, and to yield better performance facing high-dimensional data. An iterative algorithm based on block coordinate descent scheme was formulated to efficiently find a local optimizer. Extensive classification experiments on synthetic, real-world, and high-dimensional datasets demonstrated that the SFP performance is competitive with state-of-the-art algorithms such as random forest and SVM. Our method has a major advantage over such methods in that it not only leads to a flexible nonlinear model but also can exploit any loss function in training phase without compromising computational efficiency.

Keywords: Supervised k-means, Entropy-based Fuzzification, Feature Weighting, Soft Subspace Clustering.

1. Introduction

K-means algorithm (MacQueen et al., 1967) and its variations are well-known and widely used in many unsupervised applications such as clustering and representation learning due to their simplicity, efficiency, and ability to handle large datasets. There exist many algorithms, e.g., fuzzy c-means (FCM) (Bezdek, 1981) or maximum-entropy clustering (Rose et al., 1990), extending k-means such that the resulting

*Graduated M.Sc., email: p.ashtari@alum.sharif.edu

†Graduated M.Sc., email: f.nateghi@aut.ac.ir

‡email: beigy@sharif.edu

partition becomes fuzzy, i.e, data points can belong to more than one cluster. Some other extended versions of k-means employ a feature weighting approach, considering weights for features and estimating them, allowing determination of significant features (Friedman and Meulman, 2004; Huang et al., 2005; Jing et al., 2007). This approach is often followed in the context of soft subspace clustering, which can also be useful when it comes to high-dimensional data that have most of its information in a subset of features rather than all features.

On the other hand, few efforts have been made in order to generalize k-means to be suitable for supervised problems. The majority of relevant methods aimed at modifying k-means to the case of semi-supervised clustering, where the number of labeled data points is relatively small, causing them to become computationally intractable or their performance to get worse when it comes to fully-supervised tasks. Moreover, such methods typically employ Euclidean distance, which becomes less informative as the number of features grows, making them inefficient in high-dimensional scenarios.

In this paper, we propose a supervised, generative algorithm derived from k-means, called supervised fuzzy partitioning (SFP), that benefits from labels and the loss function by incorporating them into the objective function through a penalty term being a surrogate for the empirical risk. We also employ entropy-based regularizers both to achieve a fuzzy partition and to learn weights of features, yielding a flexible nonlinear model capable of selecting significant features and performing more effectively dealing with high-dimensional data. We verify the efficiency and superiority of the SFP in classification through experiments on synthetic and real-word datasets. The results demonstrate that the performance of the proposed algorithm is competitive with effective methods such as random forest and SVM.

The rest of this paper is organized as follows: Section 2 briefly reviews related techniques in incorporation of supervision into centroid-based methods. Section 3 presents the SFP algorithm. Experiments are presented in Section 4. We conclude this paper in Section 5.

2. Related Work

There have been many methods successfully modifying k-means to make use of side information when a small number of data points are labeled. Such methods have been widely studied in semi-supervised clustering (SSC) literature. One of the most popular frameworks to incorporate supervision is the constraint-based approach in which constraints resulted from existing labels are involved in a clustering algorithm to achieve a more appropriate data partitioning. This is done, for example by enforcing constraints during clustering (Wagstaff et al., 2001), initializing and constraining clustering according to labeled data points (Basu et al., 2002), or imposing penalties for violation of constraints (Basu et al., 2004a,b; Bilenko et al., 2004). These algorithms typically use pairwise *must-link* and *cannot-link* constraints between points in a dataset according to the provided labels. Given a set of data points $\{\mathbf{x}_1, \dots, \mathbf{x}_n\} \subseteq \mathbb{R}^p$, let \mathcal{M} be a set of must-link pairs such that $(\mathbf{x}_i, \mathbf{x}_{i'}) \in \mathcal{M}$ implies \mathbf{x}_i and $\mathbf{x}_{i'}$ should be in the same cluster, and \mathcal{C} be a set of cannot-link pairs such that $(\mathbf{x}_i, \mathbf{x}_{i'}) \in \mathcal{C}$ implies \mathbf{x}_i and $\mathbf{x}_{i'}$ should not be in the same cluster.

PCKMeans (Basu et al., 2004a) as a representative algorithm of constraint-based framework seeks to minimize the following objective function:

$$\mathcal{J}_{\text{PCKMeans}} = \sum_{i=1}^n \|\mathbf{x}_i - \mathbf{v}_{c_i}\|^2 + \sum_{(\mathbf{x}_i, \mathbf{x}_{i'}) \in \mathcal{M}} \alpha_{ii'} \mathbb{1}(c_i \neq c_{i'}) + \sum_{(\mathbf{x}_i, \mathbf{x}_{i'}) \in \mathcal{C}} \bar{\alpha}_{ii'} \mathbb{1}(c_i = c_{i'}) \quad (1)$$

where c_i is the cluster assignment of a data point \mathbf{x}_i , and $A = \{\alpha_{ii'}\}$ and $\bar{A} = \{\bar{\alpha}_{ii'}\}$ are the costs of violating the constraints in \mathcal{M} and \mathcal{C} , respectively. In general, A and \bar{A} are not available, so for simplicity their all elements are assumed to have the same constant value α , which causes all constraint violations to be treated equally. However, the penalty for violating a must-link constraint between distant points should be higher than that between nearby points. Another major approach, which does not have this limitation, is based on metric learning, where the metric employed by an existing clustering algorithm is adapted such that the available constraints become satisfied. This can be done through a two-step process, e.g., first, a Mahalanobis distance can be learned from pairwise constraints (Xing et al., 2003; Davis et al., 2007; Weinberger and Saul, 2009; Koestinger et al., 2012; Mignon and Jurie, 2012), and then a modified k-means with that metric is formulated. Bilenko et al. (2004) combined both of these techniques into a single model, i.e., they used pairwise constraints along with unlabeled data for simultaneously constraining the clustering and learning distance metrics in a k-means-like formulation.

One major drawback of both approaches is that they typically need pairwise information, which in turn, requires intensive computations and storage when the number of labeled data points grows, making them impractical for large datasets. Moreover, they do not take into consideration the loss function by which the predictions are to be evaluated, thus their performance can become worse for example in situations that predicted labels for test data are evaluated by a loss function different from classification rate. Overall, these methods are aimed at semi-supervised scenarios, where the number of labeled data points is relatively small, rather than supervised scenarios.

On the other hand, few efforts have been made in order to generalize k-means to be suitable for supervised problems. Al-Harbi and Rayward-Smith (2006) involved simulated annealing scheme to find the optimal weights based on labels in a modified k-means employing weighted Euclidean metric. In contrast to many soft subspace clustering algorithms with feature weighting approach, there is not an analytical solution for weights in each iteration, and the algorithm updates weights by simulated annealing, requiring to run k-means repeatedly, which can be computationally intractable for large datasets. We propose a flexible supervised version of the centroid-based methods, with an entropy-based approach to both membership fuzzification and feature weighting, aiming at being fully scalable and effective in various settings.

3. Supervised Fuzzy Partitioning (SFP)

In this section, we first introduce a new objective function taking labels information into account in addition to within-cluster, building an optimization problem suitable

for supervised learning in Section 3.1. We then adopt a block coordinate descent (BCD) method to find a local minimizer for this problem in Section 3.2. The relation of the proposed learner with RBF network and with mixture of experts are discussed in Sections 3.4 and 3.5, respectively.

3.1. The Objective Functions of SFP

Even though centroid-based algorithms are capable of representing data points structure properly, if they are directly applied to supervised problems, poor results will be obtained since they are intended for unsupervised settings and do not involve labels information in learning procedure. We incorporate labels alongside within-cluster separation of data points into the objective function, achieving an algorithm applicable to supervised settings.

Every *fuzzy partition* of the n data points into k clusters can be represented by a *membership matrix* $\mathbf{U} = [u_{ij}]_{n \times k}$ as follows:

$$\begin{aligned} \sum_{j=1}^k u_{ij} &= 1, \quad i = 1, \dots, n, \\ u_{ij} &\geq 0, \quad i = 1, \dots, n, \quad j = 1, \dots, k. \end{aligned} \quad (2)$$

where u_{ij} expresses the membership degree of point \mathbf{x}_i in the j th cluster. By limiting the constraint $u_{ij} \geq 0$ to $u_{ij} \in \{0, 1\}$, the membership matrix will represent a *crisp partition*. In this case, u_{ij} simply indicates whether the data point \mathbf{x}_i belongs to the j th cluster or not. There are many measures of fuzziness reflecting how much uniform the distribution of membership degrees are. The entropy of memberships can be taken as a such measure, which for a membership vector $\mathbf{u} = (u_1, \dots, u_k)$ is defined as follows:

$$H(\mathbf{u}) = - \sum_{j=1}^k u_j \ln u_j. \quad (3)$$

In this paper, we use this in the proposed objective function to regulate fuzziness of membership and weight parameters.

Given a training set $\mathcal{D} = \{(\mathbf{x}_i, y_i)\}_{i=1}^n$ —where $\mathbf{x}_i \in \mathcal{X} \subseteq \mathbb{R}^p$ is an input vector, and $y_i \in \mathcal{Y} \subseteq \mathbb{R}$ is its label—and a convex loss function $\ell : \mathcal{Y} \times \mathcal{Z} \mapsto \mathbb{R}_+$, we add a regularization term to a k-means-like objective function, imposing a penalty on the empirical risk $R(\mathbf{Z}) = \frac{1}{n} \sum_{i=1}^n \ell(y_i, \sum_{j=1}^k u_{ij} \mathbf{z}_j)$, where \mathbf{z}_j is the *label prototype* of the j th cluster that we wish to estimate. By (2) and convexity of the loss function it can be easily obtained that

$$\sum_{i=1}^n \ell(y_i, \sum_{j=1}^k u_{ij} \mathbf{z}_j) \leq \sum_{i=1}^n \sum_{j=1}^k u_{ij} \ell(y_i, \mathbf{z}_j). \quad (4)$$

Note that in the case of crisp partition, the equality holds. Now, we found an upper bound for the risk, which can be used as a *surrogate term* to penalizing the empirical risk. It is expected that overall the lower the surrogate, the lower the risk (note that this does not necessarily hold always), validating the use of the surrogate in regulating the risk and consequently the amount of labels contribution.

The surrogate is particularly useful in that it is a linear combination of u_{ij} s, which in turn causes the step of memberships updating in Lloyd’s algorithm to be feasible and straightforward.

Since typical Euclidean distance becomes less informative as the number of features grows (Beyer et al., 1999; Kriegel et al., 2009), we employ weighted Euclidean distance in within-cluster term alongside a penalty on the negative entropy of weights in the way similar to EWKM (Jing et al., 2007). This regularization leads to better performance and prevents overfitting especially in high-dimensional settings. Throughout this paper, we denote the weighted Euclidean distance between data points \mathbf{x}_i and $\mathbf{x}_{i'}$ by $\|\mathbf{x}_i - \mathbf{x}_{i'}\|_{\mathbf{w}} = (\sum_{l=1}^p w_l (x_{il} - x_{i'l})^2)^{1/2}$, where \mathbf{w} is the weight vector. Similarly, we also extend conventional k-means to a fuzzy version by adding entropy-based regularization to the objective function, achieving a more flexible model. As a result, we propose a supervised, weighted, and fuzzy version of k-means, *supervised fuzzy partitioning (SFP)*, through the following problem:

$$\begin{aligned}
& \underset{\mathbf{U}, \mathbf{V}, \mathbf{W}, \mathbf{Z}}{\text{minimize}} && \sum_{j=1}^k \sum_{i=1}^n u_{ij} \|\mathbf{x}_i - \mathbf{v}_j\|_{\mathbf{w}_j}^2 + \alpha \sum_{j=1}^k \sum_{i=1}^n u_{ij} \ell(y_i, \mathbf{z}_j) \\
& && + \gamma \sum_{j=1}^k \sum_{i=1}^n u_{ij} \ln u_{ij} + \lambda \sum_{j=1}^k \sum_{l=1}^p w_{jl} \ln w_{jl} \\
& \text{subject to} && \sum_{j=1}^k u_{ij} = 1, \quad i = 1, \dots, n, \\
& && u_{ij} \geq 0, \quad i = 1, \dots, n, \quad j = 1, \dots, k, \\
& && \sum_{l=1}^p w_{jl} = 1, \quad j = 1, \dots, k, \\
& && w_{jl} \geq 0, \quad j = 1, \dots, k, \quad l = 1, \dots, p.
\end{aligned} \tag{5}$$

where the first and second term represent the within-cluster separation of data points and labels, respectively. $\alpha \geq 0$ is a hyperparameter that controls the strength of labels contribution. The greater α is, the more reliant the resulting partition will be on labels information. The third term is the negative entropy of memberships, and $\gamma > 0$ is the regularization parameter. A large γ results in uniform membership values, u_{ij} , and hence, fuzzier partition. A closer-to-zero γ makes u_{ij} converge to 0 or 1, leading to a more crisp partition. The last term is also the negative entropy of feature weights, and $\lambda > 0$ controls the distribution of weights. A large λ results in uniform weights, while a small one makes some weights close to 0, which is useful to figure out significant features. The hyperparameters α, γ, λ , and k are often tuned by cross-validation (it is further discussed in Section 4). Similar to k-means, it is computationally intractable to find a global minimizer for (5); however, we introduce an efficient algorithm in Section 3.2 that converges quickly to a local minima.

So far we have discussed the phase of parameter learning. Now, let \mathbf{x}' be a new data point, and we are to make a prediction about its label by SFP method. To do this, we first estimate the membership vector \mathbf{u}' associated with \mathbf{x}' by solving the

following problem:

$$\begin{aligned} & \underset{\mathbf{u}'}{\text{minimize}} && \sum_{j=1}^k u'_j \|\mathbf{x}' - \mathbf{v}_j\|_{\mathbf{w}_j}^2 + \gamma \sum_{j=1}^k u'_j \ln u'_j \\ & \text{subject to} && \sum_{j=1}^k u'_j = 1, \quad u'_j \geq 0, \quad j = 1, \dots, k. \end{aligned} \quad (6)$$

where \mathbf{v}_j s and \mathbf{w}_j s are those that have been calculated in training phase by (5). Centers and weights are expected not to change significantly by only adding one new data point, making it valid to use those obtained during the training phase. Furthermore, the label of the new point is unknown, causing (5) to turn into (6) for prediction phase (note that our focus is on supervised problems, and other scenarios, such as semi-supervised, are beyond the scope of this paper). Fortunately, there is a closed-form solution for (6), provided by the following theorem.

Theorem 1 *Let $S = \{\boldsymbol{\theta} \in \mathbb{R}^m \mid \sum_{i=1}^m \theta_i = 1, \theta_i \geq 0, i = 1, \dots, m\}$ be a standard simplex and $\mathbf{a} \in \mathbb{R}_+^m$, $\gamma > 0$ be constant. Consider the following problem:*

$$\boldsymbol{\theta}^* \in \arg \min_{\boldsymbol{\theta} \in S} \left\{ \sum_{i=1}^m a_i \theta_i + \gamma \sum_{i=1}^m \theta_i \ln \theta_i \right\}$$

Then, the solution is

$$\theta_i^* = \frac{\exp(-a_i/\gamma)}{\sum_{i'=1}^m \exp(-a_{i'}/\gamma)}, \quad i = 1, \dots, m.$$

Proof See Appendix A. ■

By Theorem 1, we can immediately write down the memberships of the new point as follows:

$$u'_j = \frac{\exp(-d'_j/\gamma)}{\sum_{j'=1}^k \exp(-d'_{j'}/\gamma)}, \quad j = 1, \dots, k. \quad (7)$$

where $d'_j = \|\mathbf{x}' - \mathbf{v}_j\|_{\mathbf{w}_j}^2$. Because the membership vector, \mathbf{u}' , can be interpreted as probabilities that the new point, \mathbf{x}' , belongs to clusters, it is natural to use that as weights in averaging label prototypes, \mathbf{z}_j s, obtained in (5) to predict labels. Hence, once \mathbf{u}' is computed, the label of \mathbf{x}' can be estimated by

$$\hat{y}' = \arg \min_{y \in \mathcal{Y}} \ell(y, \sum_{j=1}^k u'_j \mathbf{z}_j). \quad (8)$$

Choosing proper loss function depends on the type of a problem and procedure of evaluation. For example, if we are given a dataset, and the prediction will be scored by hinge loss, it is reasonable to employ the hinge loss in SFP (5). In general, one can use *logloss* and *squared error* (SE) as representative loss functions for classification and regression, respectively. It is worthwhile to mention that

after estimating the parameters, one can also form the *distance matrix* $\mathbf{D} = [d_{ij}]$, where $d_{ij} = \|\mathbf{x}_i - \mathbf{v}_j\|_{\mathbf{w}_j}^2 + \alpha\ell(y_i, \mathbf{z}_j)$, as a new representation of data to generate informative features. Particularly, in the case of $k < p$, the representation leads to a supervised dimensionality reduction procedure. In this paper, we only consider classification scenario.

3.2. Block Coordinate Descent for SFP

Block coordinate descent (BCD) algorithms solving k-means-like problems go back to (MacQueen et al., 1967). The BCD is based on the divide-and-conquer idea that can be generally utilized in a wide range of optimization problems. It operates by partitioning variables into disjoint blocks and then iteratively optimizes the objective function with respect to variables of a block while all others are kept fixed.

Having been inspired by the conventional k-means algorithm (Hartigan, 1975; Hartigan and Wong, 1979), we develop a BCD-based scheme in order to find a local minimum for SFP problems (5). Consider four blocks of parameters: memberships (\mathbf{U}), centers (\mathbf{V}), label prototypes (\mathbf{Z}), and weights \mathbf{W} . Starting with initial values of centers, label prototypes, and weights, in each step of a current iteration, three of the blocks are kept fixed, and the objective function is minimized with respect to the others. One can initialize parameters by randomly choosing k observations $\{(\mathbf{x}_{i_j}, y_{i_j})\}_{j=1}^k$ from the training set and uses data points $\{\mathbf{x}_{i_j}\}_{j=1}^k$ as initial centers and their corresponding label prototypes, $\{\arg \min_{\mathbf{z}} \ell(y_{i_j}, \mathbf{z})\}_{j=1}^k$, as initial label prototypes. Weights can be simply initialized from uniform distribution, i.e. $w_{jl} = 1/p$.

In the first step of an iteration, where centers, prototypes, and weights are fixed, the problem becomes

$$\begin{aligned} & \underset{\mathbf{U}}{\text{minimize}} && \sum_{j=1}^k \sum_{i=1}^n u_{ij} d_{ij} + \gamma \sum_{j=1}^k \sum_{i=1}^n u_{ij} \ln u_{ij} \\ & \text{subject to} && \sum_{j=1}^k u_{ij} = 1, \quad i = 1, \dots, n, \\ & && u_{ij} \geq 0, \quad i = 1, \dots, n, \quad j = 1, \dots, k. \end{aligned} \quad (9)$$

where $d_{ij} = \|\mathbf{x}_i - \mathbf{v}_j\|_{\mathbf{w}_j}^2 + \alpha\ell(y_i, \mathbf{z}_j)$. Problem (9) can be viewed as n separate subproblems that each have the same form as that inspected in Theorem 1. As a result, the estimated memberships are as follows:

$$\hat{u}_{ij} = \frac{\exp(-d_{ij}/\gamma)}{\sum_{j'=1}^k \exp(-d_{ij'}/\gamma)}, \quad i = 1, \dots, n, \quad j = 1, \dots, k. \quad (10)$$

The intuition is that if the i th observation is close to the j th cluster, i.e. d_{ij} is small, then (10) leads to the higher degree of membership, \hat{u}_{ij} . Having computed memberships, in the second step, we can update centers of SFP by solving the

following problem:

$$\underset{\mathbf{V}}{\text{minimize}} F(\mathbf{V}) = \sum_{j=1}^k \sum_{i=1}^n u_{ij} \|\mathbf{x}_i - \mathbf{v}_j\|_{\mathbf{w}_j}^2 \quad (11)$$

assuming $\sum_{i=1}^n u_{ij} > 0$, setting the gradient of F with respect to \mathbf{v}_j equal to zero yields the center updating rule:

$$\hat{\mathbf{v}}_j = \frac{\sum_{i=1}^n u_{ij} \mathbf{x}_i}{\sum_{i=1}^n u_{ij}}, \quad j = 1, \dots, k \quad (12)$$

It is noteworthy that new centers, $\hat{\mathbf{v}}_j$ s, do not depend on weights and are updated only through data points and memberships. In parallel with centers, label prototypes are updated as follows:

$$\hat{\mathbf{z}}_j = \arg \min_{\mathbf{z} \in \mathcal{Z}} \sum_{i=1}^n u_{ij} \ell(y_i, \mathbf{z}), \quad j = 1, \dots, k. \quad (13)$$

the solution of this relies on the loss function and the memberships. For many common loss functions, such as squared error and logloss, prototype $\hat{\mathbf{z}}_j$ can be easily obtained in closed form (see Table 1). Note that according to (13), label prototypes are updated without using centers, enabling simultaneous calculation of the both blocks, which in turn makes the updating process faster. Finally, weights can be updated by applying the Theorem 1, resulting in formula analogous to that for memberships:

$$\hat{w}_{jl} = \frac{\exp(-s_{jl}/\lambda)}{\sum_{l'=1}^p \exp(-s_{jl'}/\lambda)}, \quad j = 1, \dots, k, \quad l = 1, \dots, p. \quad (14)$$

where $s_{jl} = \sum_{i=1}^n u_{ij} (x_{il} - v_{jl})^2$. Since s_{jl} represents the variance level of the l th feature in j th cluster, it is expected the greater s_{jl} is, the smaller weight will be obtained, which is consistent with equation (14). The whole algorithm of SFP for both training and test phases is summarized in Algorithm 1.

3.3. Computational Complexity of SFP

Since SFP is a supervised extension of k-means algorithm, obtained by entropy-based fuzzification of partition and adoption of two additional steps to compute the label prototypes and feature weights, it inherits the scalability of k-means-like algorithms in manipulating large datasets, becoming practical for large-scale machine learning applications. At each iteration of BCD, the time complexity of four major steps in the training phase can be investigated as follows:

- **Updating memberships.** After initializing the feature weights, the centers, and the label prototypes, a vector of cluster membership is assigned to each data point by calculating the summation $d_{ij} = \sum_{l=1}^p w_{jl} (x_{il} - v_{jl})^2 + \alpha \ell(y_i, \mathbf{z}_j)$ and then using (10). Hence, the complexity of this step is $\mathcal{O}(nk(p+r))$ operations, where r is the cost of computing the loss, $\ell(y, \mathbf{z})$. For logloss r is equal to the number of classes, M (see Table 1).

Table 1 Loss functions and their prototypes.

Loss function $(y, z) \mapsto \ell(y, z)$	Prototype $\arg \min_{\mathbf{z} \in \mathcal{Z}} \sum_{i=1}^n u_i \ell(y_i, \mathbf{z})$
classification error; $y, z \in \{1, \dots, M\}$ $\ell(y, z) = \mathbb{1}(y \neq z)$	—
logloss; $y \in \{1, \dots, M\}$, $\mathbf{z} \in \mathbb{R}^M, \sum_{m=1}^M z_m = 1$ $\ell(y, z) = -\sum_{m=1}^M \mathbb{1}(y = m) \ln z_m$	$z_m = \frac{\sum_{i=1}^n u_i \mathbb{1}(y_i = m)}{\sum_{i=1}^n u_i}$
hinge; $y \in \{-1, 1\}, z \in \mathbb{R}$ $\ell(y, z) = \max(0, 1 - yz)$	—
logistic; $y \in \{-1, 1\}, z \in \mathbb{R}$ $\ell(y, z) = \ln(1 + \exp(-yz))$	$\ln \left(\frac{\sum_{i=1}^n u_i \mathbb{1}(y_i = 1)}{\sum_{i=1}^n u_i \mathbb{1}(y_i = -1)} \right)$

- **Updating centers.** Given the membership matrix \mathbf{U} , (12) implies that $\mathcal{O}(nkp)$ operations are needed to update k centers $\mathbf{v}_1, \dots, \mathbf{v}_k$.
- **Updating label prototypes.** The cost of this step depends on the employed loss function. Let q be the cost of prototype computation (e.g., according to Table 1, q for logloss is Mn). Hence, it is clear that the complexity of this step is $\mathcal{O}(kq)$.
- **Updating feature weights.** First variances $s_{jl} = \sum_{i=1}^n u_{ij} (x_{il} - v_{jl})^2$ are computed and then weights are updated by (14), which requires $\mathcal{O}(nkp)$ operations.

As a result, the complexity of SFP becomes $\mathcal{O}(nk(2p + r)T + kqT)$, where T is the total number of iterations. In practice, SFP often converges in fewer than 30 iterations although a 10-iteration run ($T = 10$) is sufficient for most supervised applications, resulting in the time complexity becoming practically $\mathcal{O}(nkp)$. Now, consider the test phase of SFP, where we are given m points to predict their labels. For each point, the weighted Euclidean distance to estimated centers of the training phase should be calculated, which needs $\mathcal{O}(kp)$ operations. Thus, the time complexity of the test phase becomes $\mathcal{O}(mkp)$.

In terms of space complexity, SFP needs $\mathcal{O}(np)$ storage for data points; $\mathcal{O}(nk)$ for membership matrix; $\mathcal{O}(kp)$ for centers; $\mathcal{O}(kd)$ for prototypes, where d is the dimension of the label prototype space; and $\mathcal{O}(kp)$ for feature weights, adding up $\mathcal{O}(np + nk + kp + kd + kp)$ storage. During the test phase, SFP requires $\mathcal{O}(mp + mk)$ space to store test data and their memberships. In general, both the time and the space complexity of SFP are linear in the input size n . Table 2 summarizes the computational complexity of this method.

Algorithm 1: SFP algorithm

Input: $\{(\mathbf{x}_i, y_i)\}_{i=1}^n$ (training set), \mathbf{x}' (test data point), $k \geq 2$, $\alpha \geq 0$, $\gamma > 0$, $\lambda > 0$;
Output: \hat{y}' (estimated label of test data point);
// training phase
1 Initialize centers, label prototypes, and weights;
2 **repeat**
3 Update the distance matrix between training data points and centers by
 $d_{ij} = \|\mathbf{x}_i - \mathbf{v}_j\|_{\mathbf{w}_j}^2 + \alpha \ell(y_i, \mathbf{z}_j)$;
4 Update the membership matrix according to (10);
5 Update the centers and label prototypes according to (12) and (13),
 respectively;
6 Update the weights according to (14);
7 **until** *centers do not change*;
// Test phase
8 Compute the distances between test data point and centers by
 $d'_j = \|\mathbf{x}' - \mathbf{v}_j\|_{\mathbf{w}_j}^2$;
9 Compute the membership vector of test data point according to (7);
10 Make prediction using (8);

Table 2 Computational complexity of SFP.

	Time complexity	Space complexity
Training phase	$\mathcal{O}(nk(2p+r)T + kqT)$	$\mathcal{O}(np + nk + kp + kd + kp)$
Testing phase	$\mathcal{O}(mkp)$	$\mathcal{O}(mp + mk)$

3.4. SFP As a Generalized Version of RBF Network

A closer look at (7) and (8) reveals that the output prediction of SFP can be represented by a linear combination of normalized radial basis functions (RBF). To clarify this, let \mathbf{x} be an arbitrary point whose label, $\hat{y}(x)$, we wish to estimate, and consider an SFP with logistic loss function, aimed at solving a binary classification problem. In this case, (8) simplifies to

$$\hat{y}(x) = \text{sign} \left\{ \sum_{j=1}^k z_j u_j(x) \right\}, \quad (15)$$

where $u_j(x)$ is calculated by (7). Substituting in yields

$$\hat{y}(x) = \text{sign} \left\{ \frac{\sum_{j=1}^k z_j \kappa_j(\mathbf{x}, \mathbf{v}_j)}{\sum_{j=1}^k \kappa_j(\mathbf{x}, \mathbf{v}_j)} \right\}, \quad (16)$$

where

$$\kappa_j(\mathbf{x}, \mathbf{v}) = \exp \left(- \frac{\|\mathbf{x} - \mathbf{v}\|_{\mathbf{w}_j}^2}{\gamma} \right)$$

is a Gaussian RBF kernel, and $u_j(x)$ is consequently a normalized RBF. Hence, SFP is a function approximator that has a more general form than RBF networks (Moody and Darken, 1989; Haykin et al., 2009) since it uses weighted Euclidean distance rather than the typical one. We, therefore, expect SFP to be a more flexible learner, and capable of adapting to more complex data structures. Moreover, if the number of clusters, k , is set so large that each cluster contains only one or few points, then the set of centers, $\{z_j\}_{j=1}^k$, become almost identical to the set of labels, $\{y_i\}_{i=1}^n$, making the approximating function (16) can be viewed as Nadaraya-Watson kernel regression (Nadaraya, 1964; Watson, 1964). However, due to efficiently learning the weights of features, SFP suffers less from the curse of dimensionality when the number of features grows. This view is helpful in that some theoretical results for SFP can be investigated via existing results for Nadaraya-Watson kernel regression.

3.5. SFP and Mixtures of Experts

Mixtures of experts (ME) model (Jacobs et al., 1991; Jordan and Jacobs, 1994), which has been widely used in machine learning and statistics community, refers to a broad class of mixture models intended for supervised learning tasks. In this section, we study the relationship between SFP method and a generative variant of mixtures of experts (GME), originally introduced by Xu et al. (1995). The cluster-weighted models, presented later in (Gershenfeld, 1997; Ingrassia et al., 2012; Subedi et al., 2013; Ingrassia et al., 2014, 2015; Punzo and McNicholas, 2016), also follow the same framework as GME but consider further details and extensions.

Suppose that $\mathcal{D} = \{(\mathbf{x}_i, y_i)\}_{i=1}^n$ are random samples drawn from the following parametric mixture model for the joint density:

$$p(\mathbf{x}, y; \boldsymbol{\psi}) = \sum_{j=1}^k \pi_j q(\mathbf{x}; \boldsymbol{\eta}_j) f(y|\mathbf{x}; \boldsymbol{\theta}_j), \quad (17)$$

where $\boldsymbol{\psi} = (\pi_j, \boldsymbol{\eta}_j, \boldsymbol{\theta}_j)_{j=1}^k$ are parameters to be estimated; *mixing proportions* π_j are nonnegative quantities that sum to one, i.e., $\sum_{j=1}^k \pi_j = 1, \pi_j \geq 0, j = 1, \dots, k$; and $q(\mathbf{x}; \boldsymbol{\eta}_j)$ and $f(y|\mathbf{x}; \boldsymbol{\theta}_j)$ constitute element densities, typically assumed to have multivariate normal and exponential family form, respectively. The conditional density of y given \mathbf{x} is

$$p(y|\mathbf{x}; \boldsymbol{\psi}) = \sum_{j=1}^k \pi_j g_j(\mathbf{x}; \boldsymbol{\eta}_j) f(y|\mathbf{x}; \boldsymbol{\theta}_j), \quad g_j(\mathbf{x}; \boldsymbol{\eta}_j) = \frac{\pi_j q(\mathbf{x}; \boldsymbol{\eta}_j)}{\sum_{j'=1}^k \pi_{j'} q(\mathbf{x}; \boldsymbol{\eta}_{j'})}, \quad (18)$$

where $g_j(\mathbf{x}; \boldsymbol{\eta}_j)$ are referred to as the *gating function*, equivalent to the one defined in the typical version of ME introduced by Jacobs et al. (1991). Model (17) can also be represented by unobserved latent variables $h_i \in \{1, \dots, k\}$, with the discrete distribution $\mathbb{P}(h = j) = \pi_j, j = 1, \dots, k$, as follows:

$$\begin{aligned} p(y_i|\mathbf{x}_i, h_i = j) &= f(y_i|\mathbf{x}_i; \boldsymbol{\theta}_j), \\ p(\mathbf{x}_i|h_i = j) &= q(\mathbf{x}_i; \boldsymbol{\eta}_j), \\ \mathbb{P}(h_i = j) &= \pi_j. \end{aligned} \quad (19)$$

To estimate the parameters, one can take maximum likelihood approach. The regularized log-likelihood function for the collected data is

$$\ell(\boldsymbol{\psi}) = \sum_{i=1}^n \ln \left\{ \sum_{j=1}^k \pi_j q(\mathbf{x}_i; \boldsymbol{\eta}_j) f(y_i | \mathbf{x}_i; \boldsymbol{\theta}_j) \right\} + \mathcal{P}(\boldsymbol{\psi}) \quad (20)$$

where $\mathcal{P}(\boldsymbol{\psi})$ is a penalty term. A typical method to maximize this function is EM algorithm (Dempster et al., 1977). An EM iteration monotonically increases the log-likelihood function until it reaches a local maximum, and there is no guarantee that it converges to a maximum likelihood estimator. Before proceeding with EM, we need the complete log-likelihood corresponding to complete data $\mathcal{D}_c = \{(\mathbf{x}_i, y_i, h_i)\}_{i=1}^n$, computed by the following:

$$\ell_c(\boldsymbol{\psi}) = \sum_{i=1}^n \sum_{j=1}^k \mathbb{1}(h_i = j) \{ \ln \pi_j + \ln q(\mathbf{x}_i; \boldsymbol{\eta}_j) + \ln f(y_i | \mathbf{x}_i; \boldsymbol{\theta}_j) \} + \mathcal{P}(\boldsymbol{\psi}). \quad (21)$$

Given initial values $\boldsymbol{\psi}^0$, then for $t = 1, \dots, T$, the EM iteration alternates between following two steps:

- **E-step**, in which the expectation of $\ell_c(\boldsymbol{\psi})$ conditional on data and current estimates of the parameters is computed

$$\begin{aligned} Q(\boldsymbol{\psi}, \boldsymbol{\psi}^t) &= \mathbb{E}\{\ell_c(\boldsymbol{\psi}) | \mathcal{D}; \boldsymbol{\psi}^t\} \\ &= \sum_{i=1}^n \sum_{j=1}^k u_{ij}^t \{ \ln \pi_j + \ln q(\mathbf{x}_i; \boldsymbol{\eta}_j) + \ln f(y_i | \mathbf{x}_i; \boldsymbol{\theta}_j) \} + \mathcal{P}(\boldsymbol{\psi}), \end{aligned} \quad (22)$$

where

$$\begin{aligned} u_{ij}^t &= \mathbb{E}\{\mathbb{1}(h_i = j) | \mathbf{x}_i, y_i; \boldsymbol{\psi}^t\} \\ &= \mathbb{P}(h_i = j | \mathbf{x}_i, y_i; \boldsymbol{\psi}^t) \\ &= \frac{\pi_j^t q(\mathbf{x}_i; \boldsymbol{\eta}_j^t) f(y_i | \mathbf{x}_i; \boldsymbol{\theta}_j^t)}{\sum_{j'=1}^k \pi_{j'}^t q(\mathbf{x}_i; \boldsymbol{\eta}_{j'}^t) f(y_i | \mathbf{x}_i; \boldsymbol{\theta}_{j'}^t)}, \quad i = 1, \dots, n, \quad j = 1, \dots, k, \end{aligned} \quad (23)$$

are posterior probabilities of memberships.

- **M-step**, which requires optimization of the function $Q(\boldsymbol{\psi}, \boldsymbol{\psi}^t)$ over the parameter space to give $\boldsymbol{\psi}^{t+1}$; that is

$$\boldsymbol{\psi}^{t+1} \in \arg \max_{\boldsymbol{\psi}} Q(\boldsymbol{\psi}, \boldsymbol{\psi}^t). \quad (24)$$

According to (22), the three blocks (π_1, \dots, π_k) , $(\boldsymbol{\eta}_1, \dots, \boldsymbol{\eta}_k)$, and $(\boldsymbol{\theta}_1, \dots, \boldsymbol{\theta}_k)$ can be updated independently. Assuming $\mathcal{P}(\boldsymbol{\psi})$ is independent of π_j (as is usually the case), update formula for mixing proportions can be easily calculated in closed form by

$$\pi_j^{t+1} = \frac{1}{n} \sum_{i=1}^n u_{ij}^t, \quad j = 1, \dots, k. \quad (25)$$

However, updating $\boldsymbol{\eta}_j$ and $\boldsymbol{\theta}_j$ depends on the element densities.

Being inspired by (Neal and Hinton, 1998), we can view EM algorithm for GME as a alternating minimization procedure on the new function

$$\begin{aligned}
J(\mathbf{U}, \boldsymbol{\psi}) &= \sum_{i=1}^n \sum_{j=1}^k u_{ij} D(\mathbf{x}_i; \boldsymbol{\nu}_j) + \sum_{i=1}^n \sum_{j=1}^k u_{ij} \ell(y_i, \mathbf{x}_i; \boldsymbol{\theta}_j) \\
&\quad + \sum_{i=1}^n \sum_{j=1}^k u_{ij} \ln u_{ij} - \mathcal{P}(\boldsymbol{\psi}),
\end{aligned} \tag{26}$$

where $\mathbf{U} = [u_{ij}]_{n \times k}$ is a membership matrix that satisfies (2); $D(\mathbf{x}_i; \boldsymbol{\nu}_j) = -\ln \pi_j - \ln q(\mathbf{x}_i; \boldsymbol{\eta}_j)$, where $\boldsymbol{\nu}_j = (\pi_j, \boldsymbol{\eta}_j)$; and $\ell(y_i, \mathbf{x}_i; \boldsymbol{\theta}_j) = -\ln f(y_i | \mathbf{x}_i; \boldsymbol{\theta}_j)$. This view of EM is addressed in the following theorem.

Theorem 2 *Starting with initial values $\boldsymbol{\psi}^0$, EM iterations for maximizing $\ell(\boldsymbol{\psi})$ are equivalent to BCD scheme for minimizing $J(\mathbf{U}, \boldsymbol{\psi})$.*

Proof See Appendix B. ■

By comparing $J(\mathbf{U}, \boldsymbol{\psi})$ with SFP objective function (5), we realize that they are closely related. In both of them, the first and second term can be interpreted as a representation of within-cluster variation and empirical risk, respectively. They both include entropy regularization terms for memberships u_{ij} . The entropy regularization term for weights in (5) is also associated with the penalty term in $J(\mathbf{U}, \boldsymbol{\psi})$. However, note that in general SFP objective function differs from $J(\mathbf{U}, \boldsymbol{\psi})$ in that it has hyperparameters α and γ for controlling the strength of risk penalty and crispness of memberships, respectively. To clarify the differences, consider, for example, the effort to derive a SFP with logloss function from (26) by setting

$$\begin{aligned}
\pi_j &= \frac{1}{k}, & q(\mathbf{x}_i; \boldsymbol{\eta}_j) &= \mathcal{N}(\mathbf{x}_i; \mathbf{v}_j, \frac{\gamma}{2} \text{diag}(w_{j1}^{-1}, \dots, w_{jp}^{-1})), \\
f(y_i | \mathbf{x}_i; \boldsymbol{\theta}_j) &= \prod_{m=1}^M z_{jm}^{\mathbb{1}(y_i=m)}, & \mathcal{P}(\boldsymbol{\psi}) &= -\frac{\lambda}{\gamma} \sum_{j=1}^k \sum_{l=1}^p w_{jl} \ln w_{jl}.
\end{aligned} \tag{27}$$

Substituting into (26), multiplying by γ , and dropping irrelevant constants; we get the following objective function:

$$\begin{aligned}
J(U, \boldsymbol{\psi}) &= \sum_{j=1}^k \sum_{i=1}^n u_{ij} \left\{ \|\mathbf{x}_i - \mathbf{v}_j\|_{\mathbf{w}_j}^2 - \frac{1}{2} \sum_{l=1}^p \ln w_{jl} \right\} + \gamma \sum_{j=1}^k \sum_{i=1}^n u_{ij} \ell_{\log}(y_i, \mathbf{z}_j) \\
&\quad + \gamma \sum_{j=1}^k \sum_{i=1}^n u_{ij} \ln u_{ij} + \lambda \sum_{j=1}^k \sum_{l=1}^p w_{jl} \ln w_{jl}.
\end{aligned} \tag{28}$$

where ℓ_{\log} is the logloss function defined in Table 1. We see that the hyperparameter α is not included, and the SFP with $\alpha = \gamma$ is obtained, and that distance even has an extra term. Hence, by easily incorporating hyperparameters into the $J(U, \boldsymbol{\psi})$,

we obtain a more general framework, called *generalized SFP*, which includes both GME and SFP as special cases, with the following optimization problem:

$$\begin{aligned}
& \underset{\mathbf{U}, \boldsymbol{\psi}}{\text{minimize}} && \sum_{i=1}^n \sum_{j=1}^k u_{ij} D(\mathbf{x}_i; \boldsymbol{\nu}_j) + \alpha \sum_{i=1}^n \sum_{j=1}^k u_{ij} \ell(y_i, \mathbf{x}_i; \boldsymbol{\theta}_j) \\
& && + \gamma \sum_{i=1}^n \sum_{j=1}^k u_{ij} \ln u_{ij} + \mathcal{P}(\boldsymbol{\psi}), \\
& \text{subject to} && \sum_{j=1}^k u_{ij} = 1, \quad i = 1, \dots, n, \\
& && u_{ij} \geq 0, \quad i = 1, \dots, n, \quad j = 1, \dots, k.
\end{aligned} \tag{29}$$

In this new framework, D and ℓ can be any nonnegative functions, and in contrast to (26), are not limited to functions described in terms of logarithms of densities. This is useful in that for some loss functions, such as hinge loss, deriving corresponding densities is complicated or not plausible (see e.g. (Franc et al.) in which a maximum-likelihood-based interpretation for SVM is presented). In this paper, we do not discuss generalized SFP with settings other than what is used in SFP.

4. Experiments

In this section, we evaluate the performance of our method in classification task using synthetic and real-world datasets. We start our experiment in Section 4.1 by testing SFP on two-dimensional synthetic datasets. In Section 4.2, after introducing the employed real UCI datasets and their main characteristics, we discuss the metric of evaluation, methods with which we compare SFP, and the procedure of hyperparameters tuning. Results are then reported, and the accuracy of the proposed method is examined. In Section 4.3, we evaluate SFP performance in high-dimensional scenarios.

4.1. Two-dimensional Data Examples

Using three simple synthetic datasets, spiral, tow-circle, and XOR, in Figure 1, we illustrate potential benefits of SFP in some scenarios as compared with RF. In each training procedure, key hyperparameters were tuned by grid search such that 5-fold cross-validation accuracy was maximized. In all simulations of this paper, we used logloss as a loss function required for SFP. Although both algorithms yield nearly 100% accuracy on these datasets, the resulted decision regions are strikingly different from each other.

In general, any smooth piece of the decision boundary generated by the RF is a half-plane perpendicular to one of the axes. As observed in Figures 1a, 1b, and 1c, decision boundaries come as expected with many sharp turns. This property of RF leads to unnatural models in some situations, and this major limitation cannot be overcome even by increasing the number of trees to grow. As observed, in the spiral dataset, an RF model with 100 trees leads to piecewise linear boundaries, and in

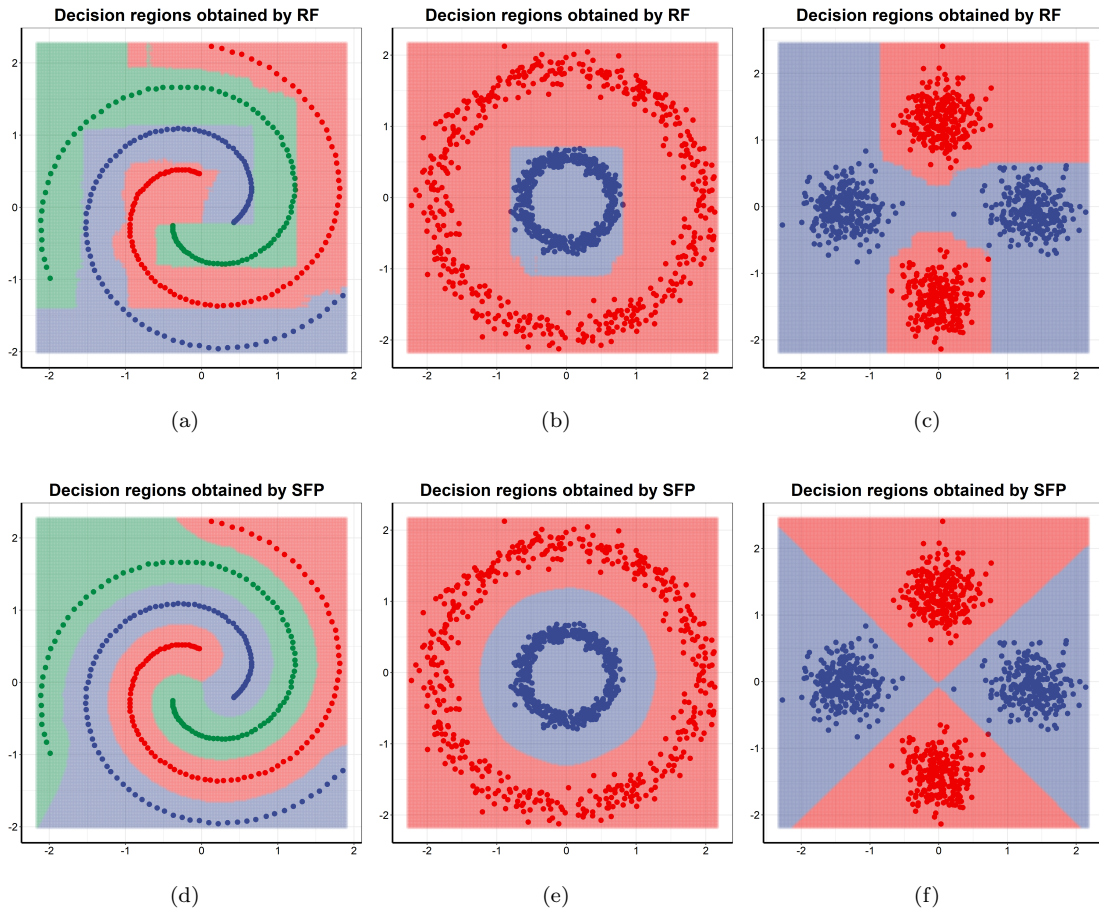


Figure 1 Decision regions on two-dimensional data. The first row shows decision regions resulted from RF on spiral, two-circle, and XOR datasets; and the second row shows corresponding decision regions resulted from SFP.

the two-circle dataset it leads to a square-shape boundary rather than a circle. In contrast, the decision boundaries obtained by SFP are much smoother.

This experiment demonstrates SFP ability in classification of nonlinear and diverse patterns through a more natural model.

4.2. Experiments on Real Data

We tested SFP on a wide range of benchmark datasets taken from the UCI machine learning repository (Dheeru and Karra Taniskidou, 2017). The characteristics of the datasets are summarized in Table 3. This collection contains data with various types, e.g., two-class, multi-class, balanced, unbalanced, categorical, continuous, and mixed.

For each dataset, first if there exists any missing data in continuous and nominal features, they were simply imputed by median and mode, respectively, and then all the nominal features were converted into numeric ones using simple dummy coding. Afterward, we normalized each feature with its mean and standard deviation. This is useful for k-means-like algorithms in that the learning process often becomes more likely to converge faster and to avoid local minima. We per-

Table 3 Characteristics of the used UCI benchmark datasets for classification.

No.	dataset	feature type	size	# features	# classes
1	abalone	mixed	4177	8	28
2	Australian	mixed	690	14	2
3	breast-cancer	continuous	699	9	2
4	cardiotocography	continuous	2126	35	10
5	Cleveland	mixed	303	13	5
6	diabetes	continuous	768	8	2
7	ecoli	continuous	336	7	8
8	hepatitis	mixed	155	19	2
9	ionosphere	continuous	351	33	2
10	iris	continuous	150	4	3
11	lymphography	mixed	148	18	4
12	parkinsons	continuous	195	22	2
13	sonar	continuous	208	60	2
14	soybean	categorical	683	35	18
15	SPECT	binary	267	22	2
16	tic-tac-toe	categorical	958	9	2
17	transfusion	continuous	748	4	2
18	vowel	mixed	990	12	11
19	wine	continuous	178	13	3
20	zoo	mixed	101	16	7

formed 5-fold cross-validation on each dataset to estimate test accuracy and repeated it 20 times to achieve reliable results. SFP was compared with representative classifiers: KNN, SVM with linear kernel (SVM-linear), SVM with RBF kernel (SVM-RBF), and random forest (RF). The `class` (Venables and Ripley, 2002), `e1071` (Dimitriadou et al., 2008), `liquidSVM` (Steinwart and Thomann, 2017), and `randomForest` (Liaw and Wiener, 2002) open source R packages have been used for KNN, SVM-linear, SVM-RBF, and RF, respectively. `e1071` provides an interface to the popular and efficient library, `LIBSVM` (Chang and Lin, 2011), for SVM. Although it supports most types of kernels, we found the new package `liquidSVM` much faster and even slightly more accurate for the case of RBF kernel. All hyperparameters were tuned via grid search guided by nested 5-fold cross-validation.

SFP algorithm has four hyperparameters $k \geq 2$, $\alpha \geq 0$, $\gamma > 0$, and $\lambda > 0$ that can be tuned by any hyperparameter optimization method. However, we simply performed a grid search on k and new parameters $\alpha' \in (0, 1]$, $\gamma' \in (0, 1)$, and $\lambda' \in (0, 1)$, where $\alpha = \frac{1-\alpha'}{\alpha'}$, $\gamma = \frac{1-\gamma'}{\gamma'}$, and $\lambda = \frac{1-\lambda'}{\lambda'}$. As a result, a reasonable search space can be $k \in \{M + i(\frac{n'-M}{4}) \mid i = 0, \dots, 4\}$, where n' is the size of training data in the cross-validation loop, and $\alpha', \gamma', \lambda' \in \{0.05 + 0.1i \mid i = 0, \dots, 9\}$. This search space results in a large number of SFP training procedures required by internal cross-validation, leading to intensive computations.

However, after empirical analysis of the impact of each hyperparameter, we found that a much smaller but effective region to search can be achieved. We demon-

strate this by applying SFP on zoo dataset and plotting 5-fold cross-validation accuracy versus each hyperparameter in Figure 2. Firstly, we observe that for a typical dataset whose size is much greater than its dimension, like zoo and others in this UCI collection, as k becomes larger and larger, the accuracy often rises steadily and then starts to decline or remain stable. Thus, we can start with $k = M$ and increase it by a specific value at a time until the accuracy stops increasing. Figure 2a illustrates this for the zoo dataset. It is also noticeable that overall for the greater γ' , the greater value of k is required to achieve higher accuracy. Furthermore, Figure 2b suggests that the optimal values of γ' are very likely to occur in the interval $(0.5, 1)$. Interestingly, as shown in 2c, assuming a fixed γ' , the optimal values of α' frequently occurs in the interval $(0, \gamma')$. In fact, for a rather large range of α' within this interval, SFP algorithm often becomes relatively stable and less sensitive to α . Finally, the effect of λ' on the performance is shown in Figure 2d. As we discussed in Section 3.1, λ is a regularization parameter that controls features contribution based on their importance. Therefore, the optimal λ' depends mostly on the data dimension (more precisely $p/\log(n)$), and larger values of λ' (small λ s) are expected for high-dimensional datasets. All in all, a practical search space for hyperparameters can be reduced to $k \in \{M + i(\frac{n'-M}{4}) \mid i = 0, \dots, 4\}$, $\gamma' \in \{0.55 + 0.1i \mid i = 0, \dots, 4\}$, $\alpha' = \gamma'/2$, and $\lambda' \in \{0.05 + 0.1i \mid i = 0, \dots, 9\}$, resulting in the number of cross-validation evaluations dropping from $5 \times 10^3 = 5000$ to $5 \times 5 \times 10 = 250$.

After evaluating the accuracies using cross-validation at a discrete grid of hyperparameters, there are several strategies to select the best hyperparameters: (1) the hyperparameters associated with the highest accuracy are selected; (2) for each hyperparameter, the average of its values associated with the $q\%$ highest accuracies are selected, where q typically is smaller than 20. (3) before employing the first strategy, the accuracies are replaced by a smoothed version obtained by a nonparametric regression method, such as LOESS (Cleveland, 1979; Cleveland and Devlin, 1988). We observed that when estimated accuracies are noisy, e.g., because of cross-validation repeats being insufficient or data being very high-dimensional, third strategy is much more efficient; hence, in our simulations, we employed the third strategy.

Convergence speed is investigated in Figure 3, where the objective functions of SFP on zoo and breast-cancer datasets over successive BCD iterations are plotted. Note that BCD has converged in fewer than 15 iterations, and overall greater reductions of the objective function are seen in the early iterations. Although the speed of convergence depends on data and initialization, in practice 30 iterations are enough for most applications.

Table 4 shows the means and standard deviations of the accuracy rate on the UCI datasets, as well as the average accuracy of each algorithm. It can be seen that SFP and SVM-linear obtained the best and the worst average accuracy, respectively. To examine whether differences are significant, a pairwise paired t-test is performed, and the p-values are reported in Table 5. Considering the significance level of 5%, the performance of SFP is superior to those of KNN and SVM-linear, but is not significantly better than those of SVM-RBF and RF. Overall, SFP, SVM-RBF, and RF yielded comparable results in terms of accuracy, but better results compared to

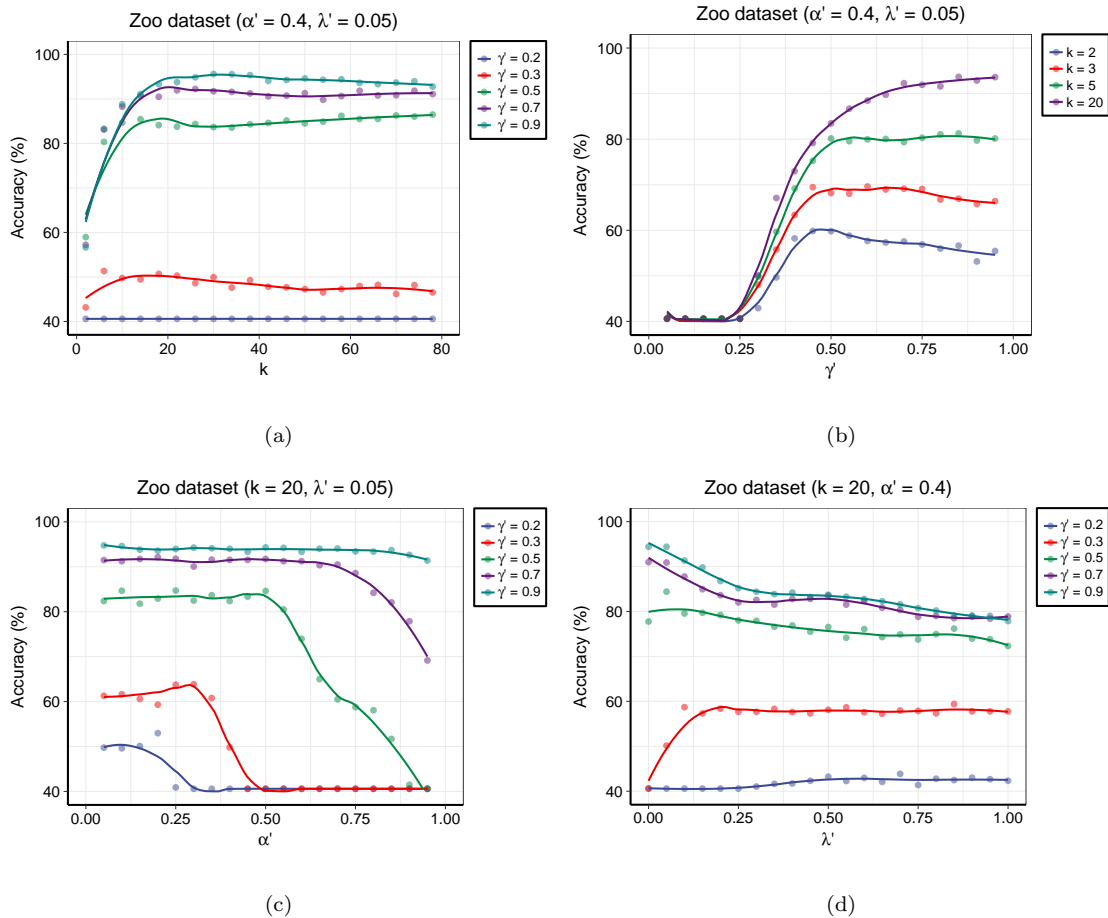


Figure 2 5-fold cross-validation accuracy of SFP on zoo dataset against hyperparameters. Figures 2a, 2c, and 2d shows plots of accuracy versus k , α' , and λ' respectively, for different values of γ' . In all plots, the smooth curves are obtained via LOESS.

KNN and SVM-linear.

4.3. Experiments on High-dimensional Data

To assess the effectiveness of our proposed classifier in high-dimensional scenarios ($p \gg n$), we used four gene expression datasets. These datasets typically contain the expression levels of thousands of genes across a small number of samples (< 200), giving information about tumor diagnosis or helping to identify the cancer type (or subtype) and the right therapy. Their specifications are briefly outlined in the following:

- Colon (Alon et al., 1999): This dataset contains 62 samples, among which 40 are from tumors and the remaining are normal. The number of genes (features) is 2000.
- Leukemia (Golub et al., 1999): This dataset contains expression levels of 7129 genes from 72 acute leukemia patients, labeled with two classes: 47 acute lymphoblastic leukemia (ALL) and 25 acute myeloid leukemia (AML).

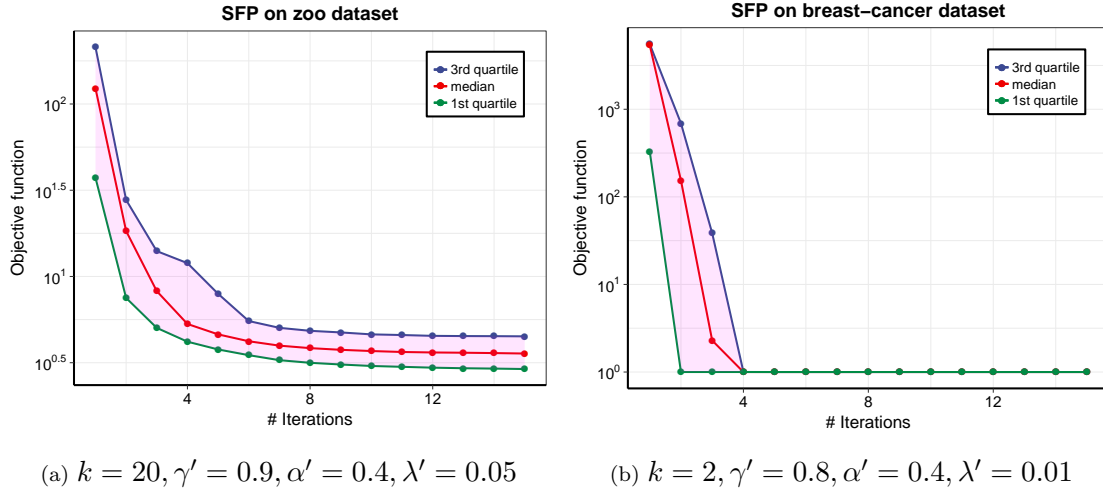


Figure 3 Evolution of the SFP objective function on zoo and breast-cancer datasets, as a function of the number of iterations. In each iteration, the three quartiles resulted from 1000 runs of the BCD are provided. To display in a logarithmic scale, the objective function is shifted such that all values become positive.

- Lung (Gordon et al., 2002): This dataset contains 181 samples, among which 31 samples are labeled with MPM and 150 labeled with ADCA. Each sample is described by 12533 genes.
- Lymphoma (Alizadeh et al., 2000): This dataset consists of 45 samples from Lymphoma patients described by 4026 genes and classified into two subtypes: 23 GCL, 22 ACL.

Similar to Section 4.2, we first scaled each dataset. To estimate generalization performance, we performed 20 runs of 5-fold cross-validation. The representative algorithms with which we compared SFP as well as the procedure of hyperparameter tuning are also the same as those used in Section 4.2. We observed that in almost all cases, for high-dimensional datasets, $k = M$ often is the best choice and become selected in hyperparameter tuning.

Since all the used gene expression datasets are two-class, and both type I and type II errors are concerned to diagnose cancer and have different consequences, in addition to accuracy, we have used several metrics, to assess the effectiveness of our method:

- Accuracy = $\frac{TP + TN}{TP + FP + FN + TN}$
- Sensitivity = $\frac{TP}{TP + FN}$
- Specificity = $\frac{TN}{TN + FP}$
- AUC: Area under receiver operating characteristic (ROC) curve

where TP, FP, FN, TN denote the number of true positives, false positives, false negatives, and true negatives, respectively. Table 6 shows the accuracy and AUC

Table 4 The 5-fold CV accuracy of the comparing algorithms (mean \pm std) on the UCI benchmark classification datasets.

dataset	KNN	SVM- linear	SVM- RBF	RF	SFP
abalone	26.6 \pm 1.8	26.3 \pm 2.1	27.6 \pm 1.5	24.9 \pm 0.7	26.4 \pm 1.2
Australian	85.7 \pm 2.8	85.4 \pm 3.1	86.0 \pm 3.0	86.9 \pm 2.9	85.6 \pm 2.5
breast-cancer	96.4 \pm 1.5	96.7 \pm 1.4	96.5 \pm 1.5	96.8 \pm 1.3	96.5 \pm 1.6
cardiotocography	98.8 \pm 0.4	98.8 \pm 0.5	99.0 \pm 0.5	98.8 \pm 0.5	98.9 \pm 0.4
Cleveland	56.9 \pm 6.2	56.7 \pm 7.3	57.2 \pm 6.5	57.5 \pm 6.7	57.0 \pm 6.8
diabetes	74.6 \pm 3.2	77.1 \pm 2.7	76.7 \pm 2.9	76.2 \pm 3.0	76.1 \pm 3.4
ecoli	84.9 \pm 4.1	86.5 \pm 4.1	85.8 \pm 4.2	86.5 \pm 4.5	86.3 \pm 3.9
hepatitis	84.5 \pm 6.1	83.8 \pm 5.9	82.5 \pm 6.1	85.2 \pm 6.1	83.4 \pm 6.0
ionosphere	85.9 \pm 4.1	87.0 \pm 3.5	90.1 \pm 3.7	93.3 \pm 2.8	92.0 \pm 3.4
iris	94.5 \pm 3.9	96.0 \pm 3.5	95.3 \pm 3.4	94.4 \pm 3.9	94.8 \pm 4.0
lymphography	81.0 \pm 6.1	85.2 \pm 6.1	82.3 \pm 6.2	83.1 \pm 7.0	82.4 \pm 6.6
parkinsons	93.4 \pm 4.6	87.0 \pm 5.0	94.3 \pm 4.3	90.2 \pm 4.8	93.8 \pm 3.9
sonar	85.3 \pm 5.7	76.5 \pm 5.9	86.9 \pm 6.1	82.6 \pm 6.0	85.2 \pm 5.7
soybean	91.5 \pm 2.3	92.7 \pm 1.9	91.7 \pm 2.4	93.7 \pm 1.7	93.0 \pm 2.2
SPECT	79.4 \pm 5.3	80.8 \pm 4.9	82.6 \pm 4.9	81.7 \pm 4.6	82.1 \pm 5.5
tic-tac-toe	100.0 \pm 0.0	98.3 \pm 0.7	100.0 \pm 0.0	99.0 \pm 0.6	99.9 \pm 0.2
transfusion	78.6 \pm 3.6	76.1 \pm 3.3	78.0 \pm 3.6	75.4 \pm 3.4	77.6 \pm 3.6
vowel	98.5 \pm 1.0	90.4 \pm 2.3	98.6 \pm 1.0	97.1 \pm 1.4	98.5 \pm 1.0
wine	95.4 \pm 3.8	97.4 \pm 2.6	96.4 \pm 2.9	97.9 \pm 2.1	97.5 \pm 2.5
zoo	94.3 \pm 5.0	94.4 \pm 4.6	93.3 \pm 5.1	94.8 \pm 4.4	95.5 \pm 4.4
average	84.3	83.7	85.0	84.8	85.1

on each dataset for comparing methods. The sensitivity versus specificity is also plotted in Figure 4a. The performance of SFP on Colon and Leukemia datasets was better than other classifiers in terms of all the four metrics. However, SVM-linear and RF outperformed the others on Lung and Lymphoma datasets. Overall, SFP leads to competitive results in case of high-dimensional data. That is mainly due to the existence of entropy regularization terms for the weights and memberships, which enables SFP algorithm to control the flexibility and complexity of the model by tuning the parameters γ and λ , and to select significant features in a way that the model suffers less from the curse of dimensionality.

In terms of running time, as we can see in Figure 4b, SFP is by far the fastest algorithm on all datasets, except the Colon, while RF is the most time-consuming in all cases. Although KNN has the minimum running time on the Colon dataset, its computational cost, in contrast to that of SFP, increases more considerably than those of other methods as the number of features or samples increases across the datasets. We have implemented SFP in R language, which is a lot slower than C++ in which other used methods are implemented; however, SFP is the clear overall winner and has significant speed advantages, especially in high-dimensional settings. This is also consistent with theoretical results for time complexity; for example one can conclude that SFP with the cost of roughly $\mathcal{O}(nkp)$ (see Section

Table 5 Pairwise comparisons using paired two-tailed t-test with unequal variances. For each pair, the method with greater average accuracy is listed first. P-values smaller than 0.05 are presented in boldface.

The pair of methods	p-value
KNN vs. SVM-linear	0.414
RF vs. KNN	0.357
RF vs. SVM-linear	0.058
SVM-RBF vs. KNN	0.026
SVM-RBF vs. SVM-linear	0.089
SVM-RBF vs. RF	0.618
SFP vs. KNN	0.029
SFP vs. SVM-linear	0.049
SFP vs. SVM-RBF	0.684
SFP vs. RF	0.307

Table 6 The 5-fold CV accuracy and AUC of the comparing algorithms on the gene expression datasets.

dataset	accuracy (%)					AUC				
	KNN	SVM-linear	SVM-RBF	RF	SFP	KNN	SVM-linear	SVM-RBF	RF	SFP
Colon	70.2	79.8	77.5	76.6	81.1	0.645	0.768	0.726	0.719	0.785
Leukemia	84.6	97.0	92.4	95.0	97.4	0.811	0.961	0.897	0.929	0.977
Lung	93.4	99.1	97.9	99.1	97.3	0.809	0.974	0.953	0.974	0.935
Lymphoma	68.0	92.7	84.3	94.2	87.7	0.683	0.926	0.844	0.942	0.876

3.2) is more efficient than SVM with the cost of $\mathcal{O}(\max(n, p) \min(n, p)^2)$ (Chapelle, 2007) in the case $k \leq \min(n, p)$, which is likely to hold in high-dimensional data.

In high dimensional settings, we expect that λ would have a critical role in achieving good performance. To see this, we first describe the procedure of feature selection based on SFP, then investigate the impact of λ on performance and resulting weights. Let $w_{jI_j(1)} \geq \dots \geq w_{jI_j(p)}$ be the feature weights of j th cluster in descending order, where $I_j(l)$ is the index of the l th largest weight of cluster j . In each cluster, We want to select the minimum number of features whose weights sum to over 0.95. More precisely, in j th cluster, the set of features $S_j = \{I_j(1), \dots, I_j(r_j)\}$ are selected, where r_j is chosen such that it holds $\sum_{l=1}^{r_j-1} w_{jI_j(l)} < 0.95 \leq \sum_{l=1}^{r_j} w_{jI_j(l)}$. Hence, the set of all significant features is $S = \bigcup_{j=1}^k S_j$. Figures 5a and 5b give a concrete example; in which, considering $k = 2$, $\gamma' = 0.6$, and $\gamma' = 0.3$, the percentage of significant features ($100 * |S|/p$) versus λ' on the Colon and the Leukemia datasets are plotted. We also illustrate AUC versus λ' in Figures 5c and 5d. For the Colon dataset, about 20% of features are significant at the optimal values of λ' , which is around 0.3, while this number for the Leukemia dataset is under 1%,

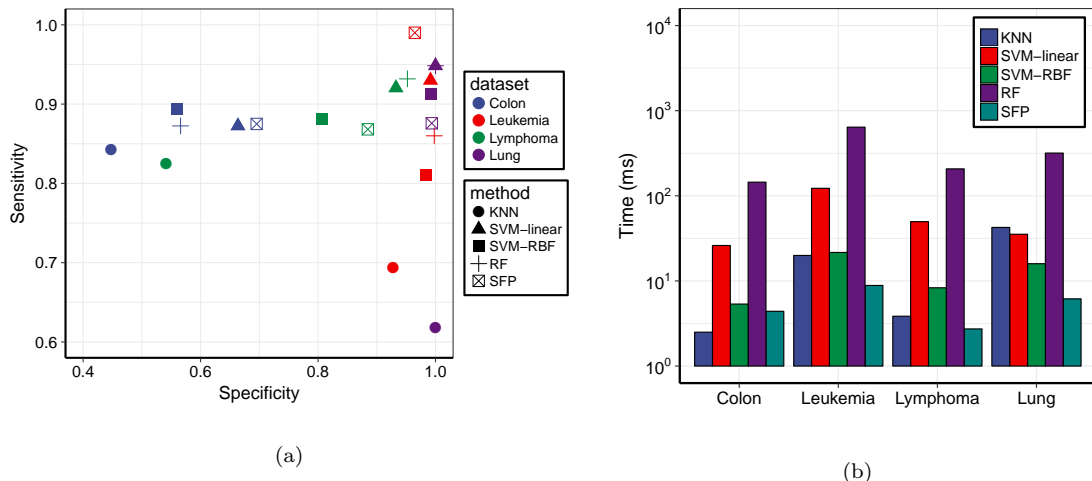


Figure 4 (a) plot of sensitivity versus specificity across the 4 gene expression datasets and the 5 methods. (b) bar plot of running time (including both training and testing time) across the 4 gene expression datasets and the 5 methods.

which occurs at $\lambda' \approx 0.9$. We see that the Leukemia dataset requires greater values of λ' , which is probably due to having over three times as many features as Colon do.

5. Conclusions

Centroid-based clustering algorithms such as fuzzy c -means (FCM) provide a flexible, simple, and computationally efficient approach to data clustering. We have extended such methods to be applicable to a wider range of machine learning tasks from classification to feature selection. Specifically, the proposed method, called supervised fuzzy partitioning (SFP), involves labels and the loss function in the k -means objective function by introducing a surrogate term as a penalty on the empirical risk. We investigated that the adopted regularization guarantees a valid penalty on the risk in case of convex loss function. The objective function was also changed such that the resulting partition could become fuzzy, which in turn made the model more complex and flexible. To achieve this, a penalty on the nonnegative entropy of memberships alongside a hyperparameter to control the strength of fuzziness were added to the objective function. To measure the importance of features and achieve more accurate results in case of high-dimensional data, we included the weights of features in the metric used in the within-cluster separation. Similar to fuzzification, we added an entropy-based regularization to limit the diversity of weights. An iterative scheme based on block coordinate descent (BCD) was presented, converging fast to a local optimizer for the SFP. Neat solutions were provided for almost all blocks, leading to fast update in an iteration. It was shown the computational complexity is linear with respect to both size and dimension. The relationship of SFP with RBF networks and mixture of experts was investigated. The SFP has a number of advantages over other centroid-based methods that use supervision: (1) in contrast to constraint-based methods, it lever-

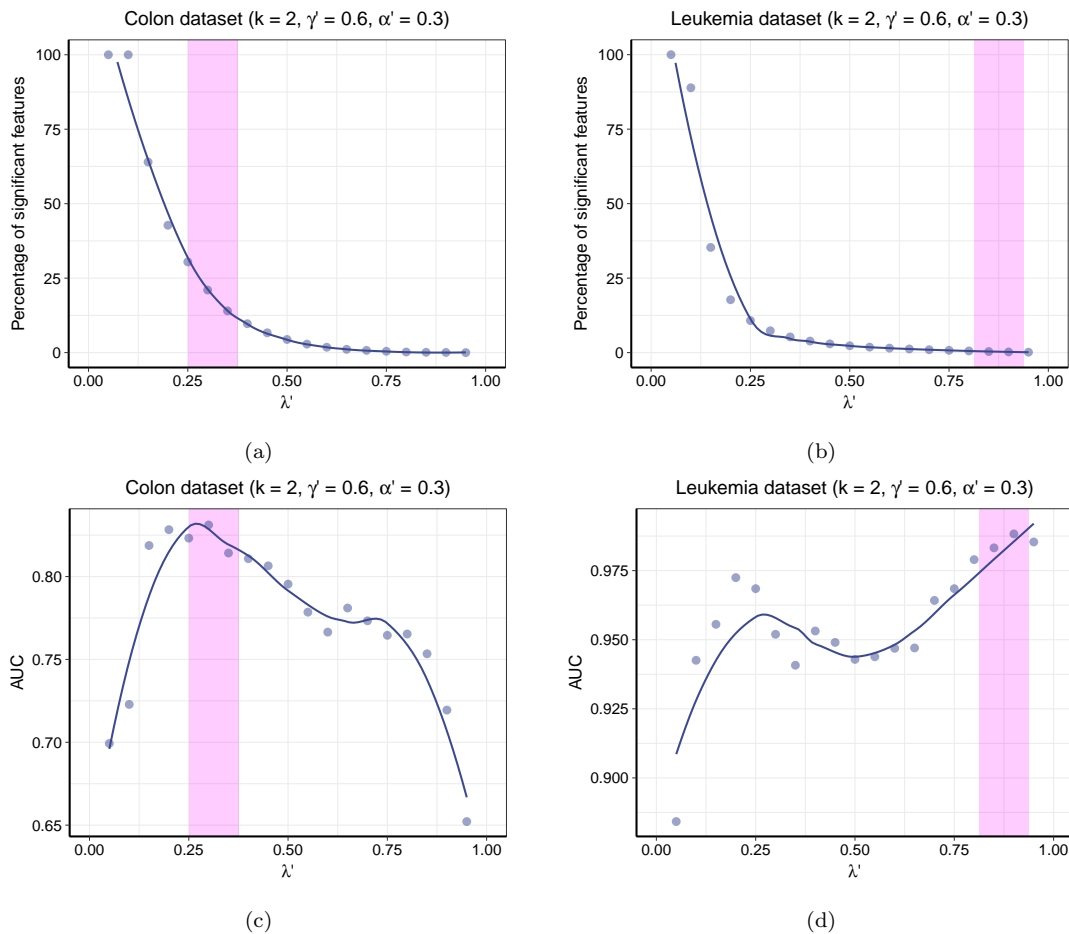


Figure 5 (a), (b) illustration of the role of λ in the selection of significant features on the colon and leukemia datasets. (c), (d) plots of AUC (estimated by 20 runs of 5-folds) versus λ' . In all plots, the smooth curves are obtained via LOESS. An interval of suitable values for λ' in terms of AUC is annotated in each plot.

ages all labeled data without a high computational cost; (2) it can use any type of loss function for employing supervision; (3) entropy-based regularizations for memberships and weights make it a very flexible model able to adapt various settings. We finally evaluated the classification performance of SFP on synthetic and real data, achieving the results competitive with random forest and SVM in terms of accuracy. Our method, in contrast to random forest, typically results in smooth decision boundaries, yielding more stable and natural models, and also can benefit from any arbitrary convex loss function profitably, and for example, unlike SVM, is not specific to hinge loss.

Appendix

A. Proof of Theorem 1

Considering the Lagrangian $L(\boldsymbol{\theta}, \lambda) = \sum_{i=1}^m a_i \theta_i + \gamma \sum_{i=1}^m \theta_i \ln(\theta_i) + \lambda(\sum_{i=1}^m \theta_i - 1)$, the first-order necessary conditions (KKT) become

$$\text{I) Stationarity: } \nabla_{\boldsymbol{\theta}} L = 0 \implies \frac{\partial L}{\partial \theta_i} = a_i + \gamma(\ln(\theta_i) + 1) + \lambda = 0, \quad i = 1, \dots, m \quad (30a)$$

$$\text{II) Feasibility: } \sum_{i=1}^m \theta_i = 1, \quad (30b)$$

These equations can be solved for the unknowns $\boldsymbol{\theta}, \lambda$. From (30) we obtain

$$\lambda^* = \gamma \ln\left(\sum_{i'=1}^m \exp\left(-\frac{a_{i'}}{\gamma}\right)\right) - \gamma, \quad (31)$$

$$\theta_i^* = \frac{\exp\left(-\frac{a_i}{\gamma}\right)}{\sum_{i'=1}^m \exp\left(-\frac{a_{i'}}{\gamma}\right)}, \quad i = 1, \dots, m, \quad (32)$$

Now, we check the second-order conditions for the problem. The Lagrangian Hessian at this point is

$$\nabla^2 L(\boldsymbol{\theta}^*, \lambda^*) = \text{diag}\left(\frac{\gamma}{\theta_1^*}, \dots, \frac{\gamma}{\theta_m^*}\right) \quad (33)$$

This matrix is positive definite, so it certainly satisfies the second-order sufficiency conditions (Luenberger et al., 1984), making $\boldsymbol{\theta}^*$ a strict local minimizer. We can also easily investigate that this problem is convex due to convexity of the objective function and the feasible region, concluding that $\boldsymbol{\theta}^*$ is also a global solution of the problem. ■

B. Proof of Theorem 2

Assume that $\boldsymbol{\psi}^t$ are estimates of the parameters at iteration t in the EM algorithm derived by (24), and that $\mathbf{U}^t = [u_{i,j}^t]$ is defined by (23); then it suffices to prove the following propositions:

- (i) $\mathbf{U}^t \in \arg \min_{\mathbf{U}} J(\mathbf{U}, \boldsymbol{\psi}^t)$
- (ii) $\boldsymbol{\psi}^{t+1} \in \arg \min_{\boldsymbol{\psi}} J(\mathbf{U}^t, \boldsymbol{\psi})$

We can show (i) simply by employing Theorem 1. If $\mathbf{U}^{t*} \in \arg \min_{\mathbf{U}} J(\mathbf{U}, \boldsymbol{\psi}^t)$, from Theorem 1, we have

$$u_{i,j}^{t*} = \frac{\exp(-D(\mathbf{x}_i; \boldsymbol{\nu}_j^t) - \ell(y_i, \mathbf{x}_i; \boldsymbol{\theta}_j^t))}{\sum_{j'=1}^m \exp(-D(\mathbf{x}_i; \boldsymbol{\nu}_{j'}^t) - \ell(y_i, \mathbf{x}_i; \boldsymbol{\theta}_{j'}^t))}$$

By substituting $D(\mathbf{x}_i; \boldsymbol{\nu}_j) = -\ln \pi_j - \ln q(\mathbf{x}_i; \boldsymbol{\eta}_j)$ and $\ell(y_i, \mathbf{x}_i; \boldsymbol{\theta}_j) = -\ln f(y_i | \mathbf{x}_i; \boldsymbol{\theta}_j)$ in the above equation and simplifying, we conclude that $u_{ij}^{t*} = u_{ij}^t$, so (i) is proved. To show (ii), we note that

$$Q(\boldsymbol{\psi}, \boldsymbol{\psi}^t) = -J(\mathbf{U}^t, \boldsymbol{\psi}) + \sum_{i=1}^n \sum_{j=1}^k u_{ij}^t \ln(u_{ij}^t),$$

and hence the problem $\arg \max_{\boldsymbol{\psi}} Q(\boldsymbol{\psi}, \boldsymbol{\psi}^t)$ is equivalent to $\arg \min_{\boldsymbol{\psi}} J(\mathbf{U}^t, \boldsymbol{\psi})$. ■

References

- Sami H Al-Harbi and Victor J Rayward-Smith. Adapting k-means for supervised clustering. *Applied Intelligence*, 24(3):219–226, 2006.
- Ash A Alizadeh, Michael B Eisen, R Eric Davis, Chi Ma, Izidore S Lossos, Andreas Rosenwald, Jennifer C Boldrick, Hajeer Sabet, Truc Tran, Xin Yu, et al. Distinct types of diffuse large b-cell lymphoma identified by gene expression profiling. *Nature*, 403(6769):503, 2000.
- Uri Alon, Naama Barkai, Daniel A Notterman, Kurt Gish, Suzanne Ybarra, Daniel Mack, and Arnold J Levine. Broad patterns of gene expression revealed by clustering analysis of tumor and normal colon tissues probed by oligonucleotide arrays. *Proceedings of the National Academy of Sciences*, 96(12):6745–6750, 1999.
- Sugato Basu, Arindam Banerjee, and Raymond Mooney. Semi-supervised clustering by seeding. In *In Proceedings of 19th International Conference on Machine Learning (ICML-2002)*. Citeseer, 2002.
- Sugato Basu, Arindam Banerjee, and Raymond J Mooney. Active semi-supervision for pairwise constrained clustering. In *Proceedings of the 2004 SIAM international conference on data mining*, pages 333–344. SIAM, 2004a.
- Sugato Basu, Mikhail Bilenko, and Raymond J Mooney. A probabilistic framework for semi-supervised clustering. In *Proceedings of the tenth ACM SIGKDD international conference on Knowledge discovery and data mining*, pages 59–68. ACM, 2004b.
- Kevin Beyer, Jonathan Goldstein, Raghu Ramakrishnan, and Uri Shaft. When is nearest neighbor meaningful? In *International conference on database theory*, pages 217–235. Springer, 1999.
- James C. Bezdek. *Objective Function Clustering*, pages 43–93. Springer US, Boston, MA, 1981.
- Mikhail Bilenko, Sugato Basu, and Raymond J Mooney. Integrating constraints and metric learning in semi-supervised clustering. In *Proceedings of the twenty-first international conference on Machine learning*, page 11. ACM, 2004.

- Chih-Chung Chang and Chih-Jen Lin. Libsvm: a library for support vector machines. *ACM transactions on intelligent systems and technology (TIST)*, 2(3):27, 2011.
- Olivier Chapelle. Training a support vector machine in the primal. *Neural computation*, 19(5):1155–1178, 2007.
- William S Cleveland. Robust locally weighted regression and smoothing scatterplots. *Journal of the American statistical association*, 74(368):829–836, 1979.
- William S Cleveland and Susan J Devlin. Locally weighted regression: an approach to regression analysis by local fitting. *Journal of the American statistical association*, 83(403):596–610, 1988.
- Jason V Davis, Brian Kulis, Prateek Jain, Suvrit Sra, and Inderjit S Dhillon. Information-theoretic metric learning. In *Proceedings of the 24th international conference on Machine learning*, pages 209–216. ACM, 2007.
- Arthur P Dempster, Nan M Laird, and Donald B Rubin. Maximum likelihood from incomplete data via the em algorithm. *Journal of the royal statistical society. Series B (methodological)*, pages 1–38, 1977.
- Dua Dheeru and Efi Karra Taniskidou. UCI machine learning repository, 2017. URL <http://archive.ics.uci.edu/ml>.
- Evgenia Dimitriadou, Kurt Hornik, Friedrich Leisch, David Meyer, and Andreas Weingessel. Misc functions of the department of statistics (e1071), tu wien. *R package*, 1:5–24, 2008.
- Vojtech Franc, Alexander Zien, and Bernhard Schölkopf. Support vector machines as probabilistic models.
- Jerome H Friedman and Jacqueline J Meulman. Clustering objects on subsets of attributes (with discussion). *Journal of the Royal Statistical Society: Series B (Statistical Methodology)*, 66(4):815–849, 2004.
- Neil Gershenfeld. Nonlinear inference and cluster-weighted modeling. *Annals of the New York Academy of Sciences*, 808(1):18–24, 1997.
- Todd R Golub, Donna K Slonim, Pablo Tamayo, Christine Huard, Michelle Gaasenbeek, Jill P Mesirov, Hilary Coller, Mignon L Loh, James R Downing, Mark A Caligiuri, et al. Molecular classification of cancer: class discovery and class prediction by gene expression monitoring. *science*, 286(5439):531–537, 1999.
- Gavin J Gordon, Roderick V Jensen, Li-Li Hsiao, Steven R Gullans, Joshua E Blumenstock, Sridhar Ramaswamy, William G Richards, David J Sugarbaker, and Raphael Bueno. Translation of microarray data into clinically relevant cancer diagnostic tests using gene expression ratios in lung cancer and mesothelioma. *Cancer research*, 62(17):4963–4967, 2002.
- John A Hartigan. Clustering algorithms. 1975.

- John A Hartigan and Manchek A Wong. Algorithm as 136: A k-means clustering algorithm. *Journal of the Royal Statistical Society. Series C (Applied Statistics)*, 28(1):100–108, 1979.
- Simon S Haykin, Simon S Haykin, Simon S Haykin, and Simon S Haykin. *Neural networks and learning machines*, volume 3. Pearson Upper Saddle River, NJ, USA., 2009.
- Joshua Zhexue Huang, Michael K Ng, Hongqiang Rong, and Zichen Li. Automated variable weighting in k-means type clustering. *IEEE Transactions on Pattern Analysis and Machine Intelligence*, 27(5):657–668, 2005.
- Salvatore Ingrassia, Simona C Minotti, and Giorgio Vittadini. Local statistical modeling via a cluster-weighted approach with elliptical distributions. *Journal of classification*, 29(3):363–401, 2012.
- Salvatore Ingrassia, Simona C Minotti, and Antonio Punzo. Model-based clustering via linear cluster-weighted models. *Computational Statistics & Data Analysis*, 71:159–182, 2014.
- Salvatore Ingrassia, Antonio Punzo, Giorgio Vittadini, and Simona C Minotti. Erratum to: The generalized linear mixed cluster-weighted model. *Journal of Classification*, 32(2):327–355, 2015.
- Robert A Jacobs, Michael I Jordan, Steven J Nowlan, and Geoffrey E Hinton. Adaptive mixtures of local experts. *Neural computation*, 3(1):79–87, 1991.
- Liping Jing, Michael K Ng, and Joshua Zhexue Huang. An entropy weighting k-means algorithm for subspace clustering of high-dimensional sparse data. *IEEE Transactions on knowledge and data engineering*, 19(8), 2007.
- Michael I Jordan and Robert A Jacobs. Hierarchical mixtures of experts and the em algorithm. *Neural computation*, 6(2):181–214, 1994.
- Martin Koestinger, Martin Hirzer, Paul Wohlhart, Peter M Roth, and Horst Bischof. Large scale metric learning from equivalence constraints. In *Computer Vision and Pattern Recognition (CVPR), 2012 IEEE Conference on*, pages 2288–2295. IEEE, 2012.
- Hans-Peter Kriegel, Peer Kröger, and Arthur Zimek. Clustering high-dimensional data: A survey on subspace clustering, pattern-based clustering, and correlation clustering. *ACM Transactions on Knowledge Discovery from Data (TKDD)*, 3(1):1, 2009.
- Andy Liaw and Matthew Wiener. Classification and regression by randomforest. *R News*, 2(3):18–22, 2002. URL <https://CRAN.R-project.org/doc/Rnews/>.
- David G Luenberger, Yinyu Ye, et al. *Linear and nonlinear programming*, volume 2. Springer, 1984.

- James MacQueen et al. Some methods for classification and analysis of multivariate observations. In *Proceedings of the fifth Berkeley symposium on mathematical statistics and probability*, volume 1, pages 281–297. Oakland, CA, USA., 1967.
- Alexis Mignon and Frédéric Jurie. Pcca: A new approach for distance learning from sparse pairwise constraints. In *Computer Vision and Pattern Recognition (CVPR), 2012 IEEE Conference on*, pages 2666–2672. IEEE, 2012.
- John Moody and Christian J Darken. Fast learning in networks of locally-tuned processing units. *Neural computation*, 1(2):281–294, 1989.
- Elizbar A Nadaraya. On estimating regression. *Theory of Probability & Its Applications*, 9(1):141–142, 1964.
- Radford M Neal and Geoffrey E Hinton. A view of the em algorithm that justifies incremental, sparse, and other variants. In *Learning in graphical models*, pages 355–368. Springer, 1998.
- Antonio Punzo and Paul D McNicholas. Parsimonious mixtures of multivariate contaminated normal distributions. *Biometrical Journal*, 58(6):1506–1537, 2016.
- Kenneth Rose, Eitan Gurewitz, and Geoffrey C Fox. Statistical mechanics and phase transitions in clustering. *Physical review letters*, 65(8):945, 1990.
- Ingo Steinwart and Philipp Thomann. liquidSVM: A fast and versatile svm package. *ArXiv e-prints 1702.06899*, feb 2017. URL <http://www.isa.uni-stuttgart.de/software>.
- Sanjeena Subedi, Antonio Punzo, Salvatore Ingrassia, and Paul D McNicholas. Clustering and classification via cluster-weighted factor analyzers. *Advances in Data Analysis and Classification*, 7(1):5–40, 2013.
- W. N. Venables and B. D. Ripley. *Modern Applied Statistics with S*. Springer, New York, fourth edition, 2002. URL <http://www.stats.ox.ac.uk/pub/MASS4>. ISBN 0-387-95457-0.
- Kiri Wagstaff, Claire Cardie, Seth Rogers, Stefan Schrödl, et al. Constrained k-means clustering with background knowledge. In *ICML*, volume 1, pages 577–584, 2001.
- Geoffrey S Watson. Smooth regression analysis. *Sankhyā: The Indian Journal of Statistics, Series A*, pages 359–372, 1964.
- Kilian Q Weinberger and Lawrence K Saul. Distance metric learning for large margin nearest neighbor classification. *Journal of Machine Learning Research*, 10(Feb):207–244, 2009.
- Eric P Xing, Michael I Jordan, Stuart J Russell, and Andrew Y Ng. Distance metric learning with application to clustering with side-information. In *Advances in neural information processing systems*, pages 521–528, 2003.

Lei Xu, Michael I Jordan, and Geoffrey E Hinton. An alternative model for mixtures of experts. In *Advances in neural information processing systems*, pages 633–640, 1995.